Supplementary Table 1

CONSORT 2010 checklist of information to include when reporting a randomised trial*

Section/Topic	Item No	Checklist item	Reported on page No
Title and abstract			
	1a	Identification as a randomised trial in the title	1
	1b	Structured summary of trial design, methods, results, and conclusions (for specific guidance see CONSORT for abstracts)	2
Introduction			
Background and objectives	2a	Scientific background and explanation of rationale	3-4
	2b	Specific objectives or hypotheses	4, 5-6
Methods			
Trial design	3a	Description of trial design (such as parallel, factorial) including allocation ratio	5
	3b	Important changes to methods after trial commencement (such as eligibility criteria), with reasons	NA
Participants	4a	Eligibility criteria for participants	5
	4b	Settings and locations where the data were collected	5
Interventions	5	The interventions for each group with sufficient details to allow replication, including how and when they were actually administered	6
Outcomes	6a	Completely defined pre-specified primary and secondary outcome measures, including how and when they were assessed	2,5-6, 7
	6b	Any changes to trial outcomes after the trial commenced, with reasons	NA
Sample size	7a	How sample size was determined	7-8
	7b	When applicable, explanation of any interim analyses and stopping guidelines	7,10, Suppl Tab 2
Randomisation:			
Sequence generation	8a	Method used to generate the random allocation sequence	6
	8b	Type of randomisation; details of any restriction (such as blocking and block size)	6
Allocation concealment mechanism	9	Mechanism used to implement the random allocation sequence (such as sequentially numbered containers), describing any steps taken to conceal the sequence until interventions were assigned	6
Implementation	10	Who generated the random allocation sequence, who enrolled participants, and who assigned participants to	6

		interventions	
Blinding	11a	If done, who was blinded after assignment to interventions (for example, participants, care providers, those assessing outcomes) and how	6
	11b	If relevant, description of the similarity of interventions	NA
Statistical methods	12a	Statistical methods used to compare groups for primary and secondary outcomes	8
	12b	Methods for additional analyses, such as subgroup analyses and adjusted analyses	8
Results			
Participant flow (a diagram is strongly recommended)	13a	For each group, the numbers of participants who were randomly assigned, received intended treatment, and were analysed for the primary outcome	9, figure 1
	13b	For each group, losses and exclusions after randomisation, together with reasons	9, figure 1
Recruitment	14a	Dates defining the periods of recruitment and follow-up	5
	14b	Why the trial ended or was stopped	9, 10, 11
Baseline data	15	A table showing baseline demographic and clinical characteristics for each group	Table 1
Numbers analysed	16	For each group, number of participants (denominator) included in each analysis and whether the analysis was by original assigned groups	8,9-12
Outcomes and estimation	17a	For each primary and secondary outcome, results for each group, and the estimated effect size and its precision (such as 95% confidence interval)	9-12
	17b	For binary outcomes, presentation of both absolute and relative effect sizes is recommended	9-10
Ancillary analyses	18	Results of any other analyses performed, including subgroup analyses and adjusted analyses, distinguishing pre-specified from exploratory	9-12
Harms	19	All important harms or unintended effects in each group (for specific guidance see CONSORT for harms)	9-11
Discussion			
Limitations	20	Trial limitations, addressing sources of potential bias, imprecision, and, if relevant, multiplicity of analyses	15
Generalisability	21	Generalisability (external validity, applicability) of the trial findings	16
Interpretation	22	Interpretation consistent with results, balancing benefits and harms, and considering other relevant evidence	13-16
Other information			
Registration	23	Registration number and name of trial registry	2,4
Protocol	24	Where the full trial protocol can be accessed, if available	5
Funding	25	Sources of funding and other support (such as supply of drugs), role of funders	18,19

*We strongly recommend reading this statement in conjunction with the CONSORT 2010 Explanation and Elaboration for important clarifications on all the items. If relevant, we also recommend reading CONSORT extensions for cluster randomised trials, non-inferiority and equivalence trials, non-pharmacological treatments, herbal interventions, and pragmatic trials. Additional extensions are forthcoming: for those and for up to date references relevant to this checklist, see www.consort-statement.org.

Supplementary Table 2. Stopping rules for the interim analysis of the SIRENA 2 trial.

Difference in favour of	**Interim analysis p-value**	**Stopping rule**
Sirolimus	$p < 0.005$	Stop the study early
Sirolimus	$p \geq 0.005$ (unless $p \geq 0.049$ and Δ excluded from the 99% CI	Complete the study as planned
Sirolimus	$p \geq 0.049$ and Δ excluded from the 99% CI	Stop the trial for futility
Conventional treatment	$p \geq 0.05$ and Δ included in the 99% CI	Stop the trial for futility (impossibility to obtain a reversal of the results at this point of the study)
Conventional treatment	$p < 0.05$ or $p \geq 0.05$ and Δ excluded from the 99% CI	Stop the trial for emerging evidence of the superiority of conventional treatment

Δ = minimum important difference of the primary end point in favour of sirolimus of 0.95 mL/min/1.73 m^2 (i.e. from -6.31 to -5.36 mL/min/1.73 m^2). 99% CI= 99% confidence interval for the difference in the primary end point

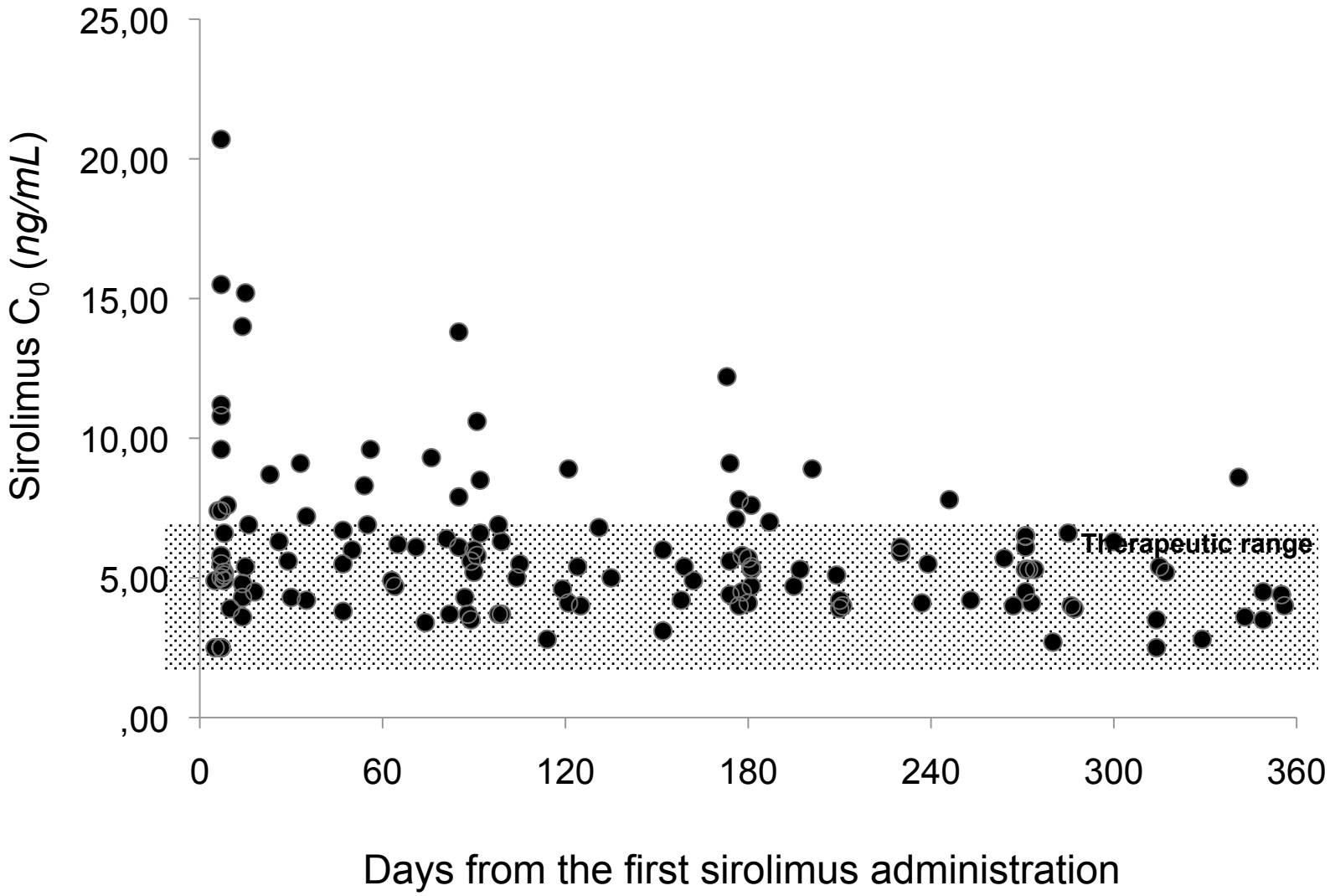

Supplemental Figure 1: Serum sirolimus levels at different time points during the study period. The gray area encompasses the therapeutic range.

Appendix 1

SIRENA 2 STUDY ORGANIZATION

Members of the SIRENA 2 Study Organization *(all in Italy unless otherwise noted):*

Principal investigator — G. Remuzzi (Bergamo, Italy); *Study coordinators* —Norberto Perico (Bergamo, Italy) and P. Ruggenenti (Bergamo, Italy); *Coordinating Center* - IRCCS - Mario Negri Institute for Pharmacological Research , Clinical Research Center for Rare Diseases Aldo e Cele Daccò , Villa Camozzi, Ranica (Bergamo, Italy); *Partecipating Center* - G. Remuzzi, N. Perico, P. Ruggenenti, M. Trillini, S. Rota, S. Prandini, V. Lecchi, G. Gherardi, L. Barcella, G. Fasolini (Azienda Ospedaliera Papa Giovanni XXIII, Unit of Nephrology and Dialysis, and Unit of Radiology, and Clinical Research Center for Rare Diseases Aldo e Cele Daccò of the IRCCS - Mario Negri Institute for Pharmacological Research); *Monitoring and Drug Distribution* (Mario Negri Institute) - N. Rubis, O. Diadei, A. Villa; *Database and Data Validation* (Mario Negri Institute) - D. Martinetti, S. Carminati, B. Ene-Iordache; *Data Analysis* (Mario Negri Institute) - A. Perna, A. Russo, G. Gentile and G. A. Giuliano; *Medical Imaging* (Mario Negri Institute) – A. Remuzzi, A. Caroli, L. Antiga, K. Sharma, C. P. Ferrer Siles, J. A. Reyes Loaeza and M. C. Aparicio; *Laboratory Measurements* (Mario Negri Institute) – F. Gaspari, F. Carrara and M. Cortinovis ; *Regulatory Affairs* (Mario Negri Institute) – P. Boccardo and S. Peracchi; *Data and Safety Monitoring Board* – E. Porrini MD (Hospital Universitario de Canarias, Tenerife, Spain), A. Schieppati MD (Ethics Committee, Ospedale Papa Giovanni XXIII, Bergamo), Alejandro Jiménez Sosa StatSciD (Hospital Universitario de Canarias, Tenerife, Spain)

Appendix 2

CT Image Acquisition and Kidney Volumes measurement

CT images were acquired with a 64-slice CT scanner (LightSpeed VCT; GE Healthcare, Milwaukee, WI). A single breath-hold scan (120 kV; 150 to 500 mAs; matrix 512x512; collimation 2.5 mm; slice pitch 0.984; increment 2.5 mm) was initiated 80 seconds after the injection of 100 ml non-ionic iodinated contrast agent (Iomeron 350; Bracco, Italy) at a rate of 2 ml/s, followed by 20 ml physiologic solution at the same injection rate. Once acquired, images were transferred in DICOM 16-bit format from the clinical scanner on digital media for subsequent processing (18) (Appendix 2). Height-adjusted TKV (ht-TKV) was computed by dividing TKV by individual patient height (19). Kidneys were first manually outlined on all acquired digital images by trained operators, who were blind to treatment, using an interactive image editing software (ImageJ, Image processing and Analysis in Java, National Institutes of Health, http://rsbweb.nih.gov/ij/). Main renal blood vessels and hilum were carefully excluded from the outlines, and special attention was given to regions where kidneys and liver were adjacent. Tracing accuracy was double-checked and, whenever needed, manual outlines were corrected by a single operator (K.S.), also blind to treatment, in order to limit potential inter-operator variability. Renal masks were created from manual outlining, and TKV was computed by multiplying the voxel count of the masks by voxel volume, as determined by the acquisition protocol. Volume computation was performed with in-house software based on the Insight Toolkit version 4.5 and developed in the C++ programming language.

Appendix 3

ADDITIONAL VOLUMETRIC ANALYSES

Renal cyst and parenchyma volumes were computed on all contrast-enhanced CT images, on the basis of manually traced kidney outlines, using a volumetric quantification method previously described in detail (Antiga 2006), and adopted in previous ADPKD clinical trials (Ruggenenti 2005, Perico 2010). Briefly, anisotropic diffusion filtering was first used to remove noise while preserving relevant features, such as the boundary between cysts and parenchyma. A histogram-based statistical classification method known as Otsu's thresholding (Otsu 1979*)* was then used to subdivide the outlined kidneys into tissue classes, so as to maximize the between class variance of image intensity values.

As patients involved in the current study had severe renal insufficiency, the exposure to the radiocontrast agent was minimized in order to prevent the risk of contrast nephrotoxicity. Because of this approach, however, some contrast-enhanced CT images were noisy and/or not enough contrasted to reliably differentiate cyst and parenchyma volumes. Moreover, some patients had hemorrhagic cysts (appearing bright on contrast-enhanced CT images), which confounded the tissue classification. For the above reasons, in this patient cohort, renal tissue segmentation required a number of additional processing steps.

Preliminary to Otsu's thresholding, all available acquisitions (n=60) underwent acquisition-specific tuning of the enhancement parameters. Six out of 60 acquisitions did not require any additional step. Twenty acquisitions, displaying up to 5 well-defined misclassified hemorrhagic cysts, required manual correction of the segmented images. On the remaining 34 acquisitions, renal cyst could not be computed due to the presence of several (more than 5) hemorrhagic cysts and heavy mix-up in the classified images, which could not be reliably manually corrected. On 15 out of these 34 acquisitions, parenchymal volume was identified by thresholding enhanced images based on a fixed

threshold (≥ 74 Hounsfield Units), defined as average parenchymal intensity on acquisitions with no processing problems; on 9 additional acquisitions, thresholding was followed by manual correction, in order to change label of well-defined hemorrhagic cysts misclassified as parenchyma. On the remaining 10 acquisitions parenchymal volume could not be reliably identified, and only total kidney volume could be computed.

From the segmented images, cyst and parenchymal volumes were computed by multiplying the voxel count of each class by voxel volume, as determined by the acquisition protocol. All image processing steps were performed with in-house software based on Insight Toolkit version 4.5 (Ibanez 2005) and developed in the C++ programming language. Manual correction of the classified images was performed with 3DSlicer (Fedorov 2012), using the editor Module.

For each tissue component, only patients with available baseline and 12-month follow-up volume data were included in the analyses.

Both renal cyst and parenchymal volumes did not significantly increase during 12 months of Sirolimus (cyst: from 1604 ± 727 to 1764 ± 831 mL, p=0.18, n=4; parenchyma: from 222 ± 59 to 233 ± 59 ml, p=0.64, n=7) or conventional therapy (cyst: from 1224 ± 482 to 1277 ± 533 mL, p=0.086, n=6; parenchyma: from 190 ± 36 to 201 ± 52 mL, p=0.32, n=9). (Figure A-1).

Figure A-1. Individual cyst (Panel A), and parenchymal (Panel B) volume volumes at baseline at at 12 months of follow-up in the two treatment groups. Horizontal thick segments denote mean values.

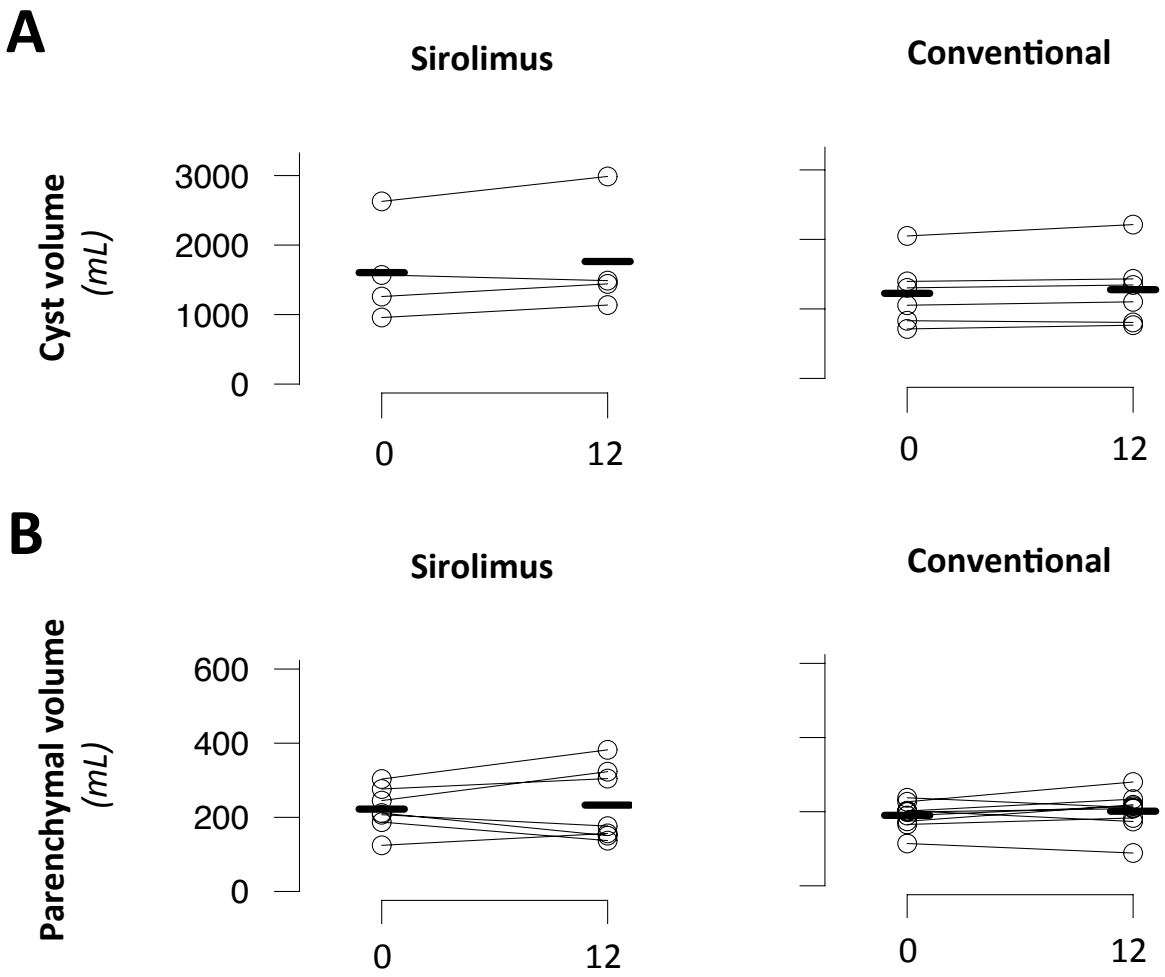

REFERENCES

A-1 Antiga L, Piccinelli M, Fasolini G, Ene-Iordache B, Ondei P, Bruno S, Remuzzi G, Remuzzi A: Computed tomography evaluation of autosomal dominant polycystic kidney disease progression: A progress report. Clin J Am Soc Nephrol 2006; 1: 754–760

A-2 Ruggenenti P, Remuzzi A, Ondei P, Fasolini G, Antiga L, Ene-Iordache B, Remuzzi G, Epstein FH. Safety and efficacy of long-acting somatostatin treatment in autosomal-dominant polycystic kidney disease. Kidney Int. 2005; 68:206-216.

A-3 Perico N, Antiga L, Caroli A, Ruggenenti P, Fasolini G, Cafaro M, Ondei P, Rubis N, Diadei O, Gherardi G, Prandini S, Panozo A, Bravo RF, Carminati S, De Leon FR, Gaspari F, Cortinovis M, Motterlini N, Ene-Iordache B, Remuzzi A, Remuzzi G. Sirolimus therapy to halt the progression of ADPKD. J Am Soc Nephrol. 2010; 21(6):1031-1040.

A-4 Otsu N: A threshold selection method from gray-level histogram. IEEE Trans Syst Man Cybern 1979; 9: 62–66

A-5 Ibanez L, Schroeder W, Ng L, Cates J: The ITK Software Guide, 2nd Ed., Albany, Kitware Inc., 2005

A-6 Fedorov A., Beichel R., Kalpathy-Cramer J., Finet J., Fillion-Robin J-C., Pujol S., Bauer C., Jennings D., Fennessy F., Sonka M., Buatti J., Aylward S.R., Miller J.V., Pieper S., Kikinis R. 3D Slicer as an Image Computing Platform for the Quantitative Imaging Network. Magn Reson Imaging. 2012; 30: 1323-1341.